https://doi.org/10.2352/ISSN.2470-1173.2019.7.IRIACV-453

Automated optical inspection for abnormal-shaped packages

Wei-Yu Lin, Chen-Tao Hsu, Chi-Chun Chang, Jen-Hui Chuang;
Department of Computer Science, National Chiao Tung University of Hsinchu, Taiwan,

Abstract

In this paper, we develop an automated optical inspection method to detect yarn packages' defect. Although textile industry is regarded as a traditional industry, many new technologies, e.g., computer vision detection algorithms, are applied to this industry in recent years. Yarn packages are the semi-finished good of textile industry. Various factors may cause abnormal-shaped packages. In this study, we develop three defect detection algorithms to extract abnormal-shape packages. These algorithms can help manufacturer to avoid the disadvantages of human inspection effectively and improve the productive quality.

Introduction

In the past, textile industry is considered as a traditional industry. Although many production procedures in the industry have been automated, defect detection still relies on human visual inspection. However, human visual inspection has disadvantages of hard to standardize and quantify. Therefore, we develop an automated optical inspection(AOI) for the manufactory to improve the accuracy of defect detection.

The AOI technology had been applied in different kinds of industry for defect detection, e.g., printed circuit board or semiconductor [1][2]. In textile industry, some AOI technologies had been applied on defect of clothes [3][4]. In this study, we develop a defect detection algorithm for packages which are the semi-finished good of textile industry.

Two factors which could cause abnormal-shaped defects. One is associated with the procedure of package producing. When the tension of winding machine is abnormal, the unbalanced winding will cause a package to have abnormal shapes, including saddle or bulge. Another factor is simply dropping or colliding when moving packages, which also causes the defect of abnormal shape. The abnormal-shaped package could cause the cloth defects during procedure of production. In this study, we will introduce a computer vision detection method to detect the packages of abnormal shape.

The rest of paper is described as follows: In Section 2, we illustrate the proposed method to calibrate the position of tested packages. In Section 3, we illustrate the methods of defect detection. In Section 4, we present the detection results of packages' defects. Finally, in Section 5, some conclusion remarks are provided.

Calibration of package position

The shape of a yarn package looks like a cylinder. Fig.1 shows the image capturing geometry in this study. The flowchart of package's defect detection is shown in Fig.2. To get better results of defects detection, we need to calibrate the package's position before detection. To that end, we use the image bilateral symmetry of package to calibrate the position. It is assumed that the original of image coordinate system is the center of image where the optical axis passes through the image plane. A normal-package's left- and right-edge will be symmetric with respect to their middle line which is linear and aligned to the vertical axis of image plane.

Thus, we have the following calibration procedures (see Fig.3):

1. Calculate edge information by Sobel operators.
2. Extract of package edge points with a fixed threshold value.
3. Calculate the middle points of left and right edge in each vertical position. The set of middle points is the middle line (L_{me}) of package's edge.
4. Calculate the sum of difference (S_d) between L_{me} and vertical axis of image plane.
5. Move the package along the horizontal axis and find the minimum of S_d.

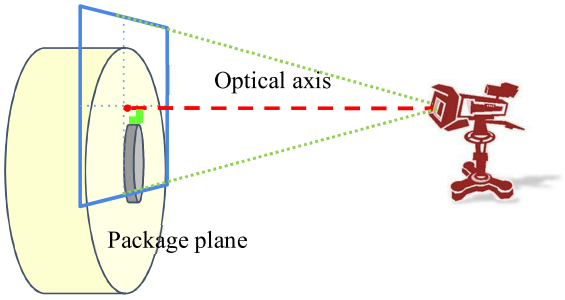

Fig.1. Image-capturing of package

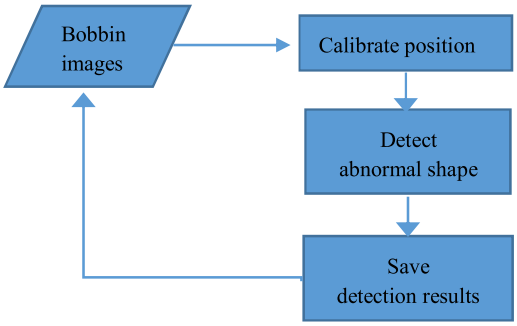

Fig.2. The flowchart of abnormal package's defect detection.

Abnormal-shaped package detection

Two factors could cause abnormal-shaped defect. The first factor is dropping or colliding when moving package. The damage causes the defect of asymmetrical-shaped packages, as shown in Fig. 4. In this study, we use the middle line of the both side of edge to detect this defect, which is not a straight line for the abnormal (asymmetric) package shape, as shown as red box in Fig.4.

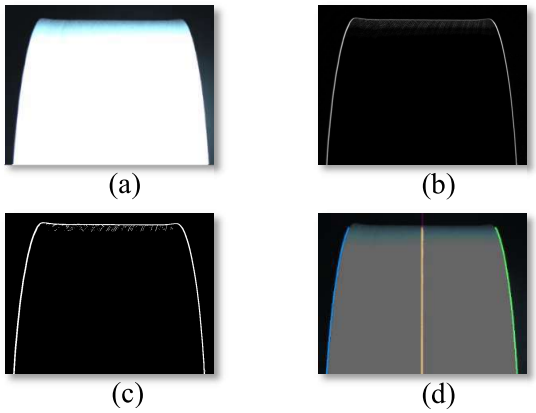

Fig.3. The procedure of calibration package position. (a) Original image, (b) edge image, (c) bi-level image, (d) middle line of edge (yellow line)

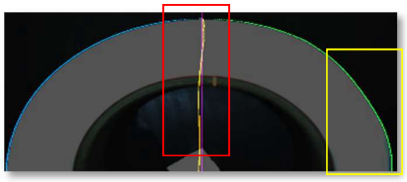

Fig.4. Abnormal shape defect of asymmetrical shapes due to collision (yellow box, bruised package).

The other defect factor is resulted from unbalanced tension during package winding, which may cause abnormal package shape including saddle or bulge. The saddle defect has abnormal shape contour from the side view of the cylindrical package, as shown in Fig. 5. The indicator of saddle defect is the difference between the highest point and the lowest point of the contour. If the difference is larger than a fixed threshold value, the package will be identified to have a saddle defect.

On the other hand, the bulge defect corresponds to abnormal shape at cross-sections of both ends of the cylindrical package. Figs.6 (a) and (b) shows the left-side image of normal and bulge packages, respectively, where one can see small differences between the two package contours. On the other hand, Figs. 6 (c) and (d) shows very much different Sobel gradient directions along the edge contours shown in Figs. 6 (a) and (b), respectively. As the edge information near the top of package image is less reliable due to the (near frontal) angle of illumination, we limit the observation range to about 2/3 of package's height, as marked in yellow in Figs. 6(a) and (b). To indicate the bulge defect, we use an exponential-fitting function to fit the profiles of gradient direction, as shown in Fig. 7. After such fitting, we calculate the average of sum-of-difference between the profile and exponential fitting curve. If the value is higher than a fixed threshold, the package is judged to a bulge defect.

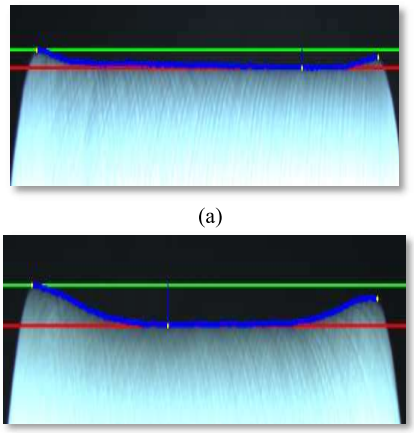

Fig.5. Examples images of (a) normal package, (b) saddle package.

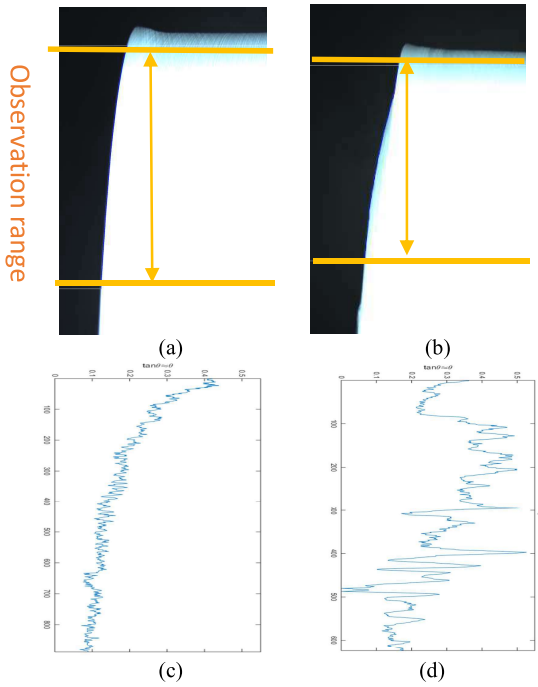

Fig. 6. Examples of normal and bulge packages. (a) and (b) are side-view images of normal and bulge packages, respectively; (c) and (d) are corresponding Sobel gradient directions.

Accordingly, we have the following bulge detection procedure:

1. Find the package position with the maximum value of gradient magnitude near by the edge of package in each height of input image.
2. Calculate the direction of image gradient at that position.
3. Establish the profile of direction of image gradient with respect to image height, as shown in blue in Fig. 7.
4. Find an exponential fitting function for such profile, as shown with dashed green line in Fig. 7.

5. If the fitting error is higher than a fixed threshold, the package is judged to have a bulge defect.

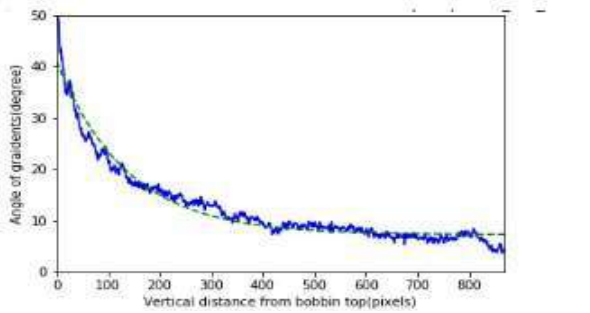

(a)

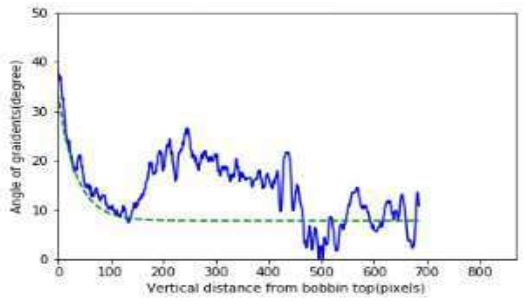

(b)

Fig. 7. The gradient direction profile of edge contour. (a) Normal package, and (b) bulge package.

In particular, we use the least-square estimation method to find the best exponential fitting function mentioned in Steps 4 and 5. In this study, we use the sum-of-difference value to measure the fitting error, while the fixed threshold value in Step 5 is decided by a statistical method which will be described in Section 4.

Experimental results

In this section, we will present some detection results of package's defects. In the experiment, we test 3 bruised packages, 3 saddle packages, 24 bulge packages, and 121 normal-shaped packages. The size of the test image is 3440×2160 pixels. We implement proposed algorithms in Intel Pentium i7-6700 CPU with 8G memory and Intel Pentium N-4200 with 4G memory. In the detection of bruised package, we use the distance between middle line, which is between left and right edges, and vertical axis to detect the defect, as shown in Fig. 4. The distances of normal-shaped and abnormal-shaped are shown in Fig. 8. If a distance value is higher than a fixed threshold, the package is considered to have bruise defect. In this study, the fixed threshold is set as 3 pixels.

For saddle defect, we measure the distance between the highest shoulder point and valley point of the package's top contour in an image, as shown in Fig. 5. The measurement results are shown in Fig. 9. Again, if the distance is higher than a fixed threshold, the package has saddle defect. In this study, the fixed threshold is set as 34 pixels. Based on the detection results, we find that some defect-free packages may have high distance value, as green area in Fig. 9. In this study, the green area is identified as an ambiguous area. Accordingly, we set a second threshold, i.e., with the black line in Fig. 9. If the distance lager than the second threshold, human inspection is needed.

As for bulge defect, we use the average of sum-of-difference value between the profile and exponential fitting curve to detect the defect. The histogram of the average sum-of-difference (SOD) in each testing package is shown in Fig. 10, with left side in (a) and right side in (b). Accordingly, we set fixed threshold values for left- and right- sides to 1.0 and 2.0 pixels, respectively, to judge the defect. The accuracy of bulge defect left and right side are 75.32 and 88.96, respectively, as shown in Table I. Again, based on the detection results, we find that some bulge-free packages may have high SOD values. For the same reason with saddle defect, we set a second threshold, as the black line in Fig. 10. If the index value falls between the black and red, human inspection will be involved.

While human inspection is still needed in the detection procedures, the proposed approach has correctly distinguished most of normal and abnormal packages. Table II lists average execution time of the three defect detections, with 0.029 seconds for bruise defect, 0.233 seconds for saddle defect, and 0.104 seconds for bulge defect. Because each defect detection is independent, if we detect three shape defects sequentially, the execution times will be added together, with a total execution time equal to about 0.366 seconds on the average.

Table I. The accuracy of bulge defect left and right side.

	TP	FN	FP	TN	Accuracy (%)
Left	22	2	37	93	75.32
Right	4	0	17	113	88.96

Table II. Average execution time for three defect detections

Detection type	Average execution time (seconds)
Colliding	0.029
Saddle	0.233
bulge	0.104

Conclusions

In this study, we apply an AOI technique to detect the abnormal-shaped defects of package, including bruise, saddle, and bulge. From our observation, it is found that the intensity variation of edge points has different characteristics between some normal and abnormal packages and can be employed to effectively detect corresponding defects of abnormal-shaped packages. On the other hand, we find that the light source is an important factor that may influence the detection results. In the future, we will focus on the relationship between light source and defect characteristics to further improve the accuracy. Besides, we will plan to build a database of package images so that big data analytics can be applied to improve the efficiency of the product line.

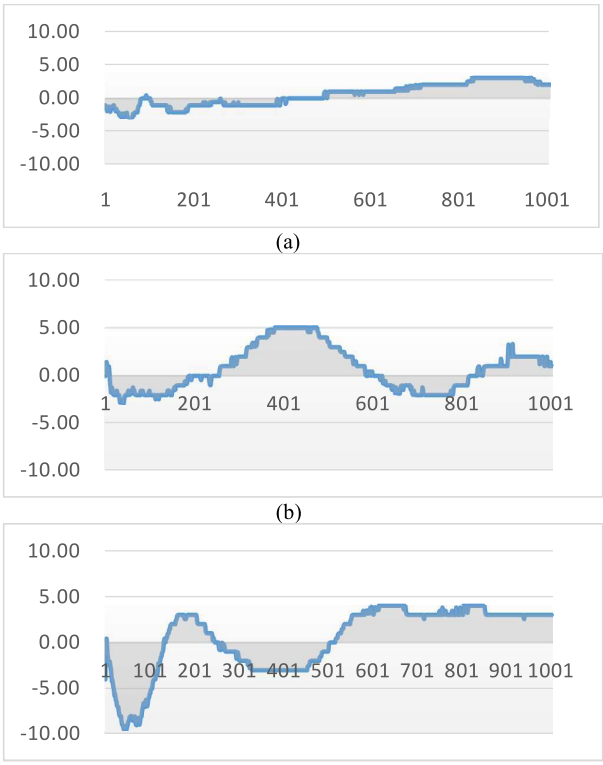

Fig.8. The distance between middle line of edge and vertical middle line of the image. (a) Normal package, (b) and (c) colliding package.

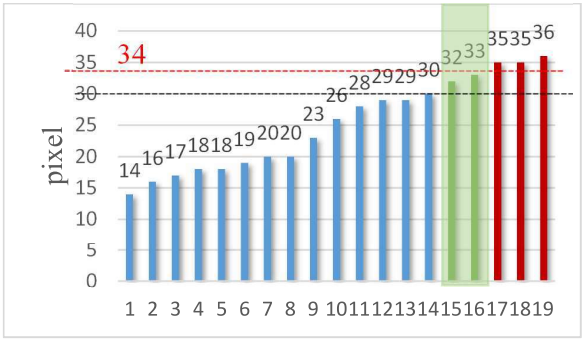

Fig.9. The measurement result of saddle defect. The green area is an ambiguous area; the black line give the second threshold value.

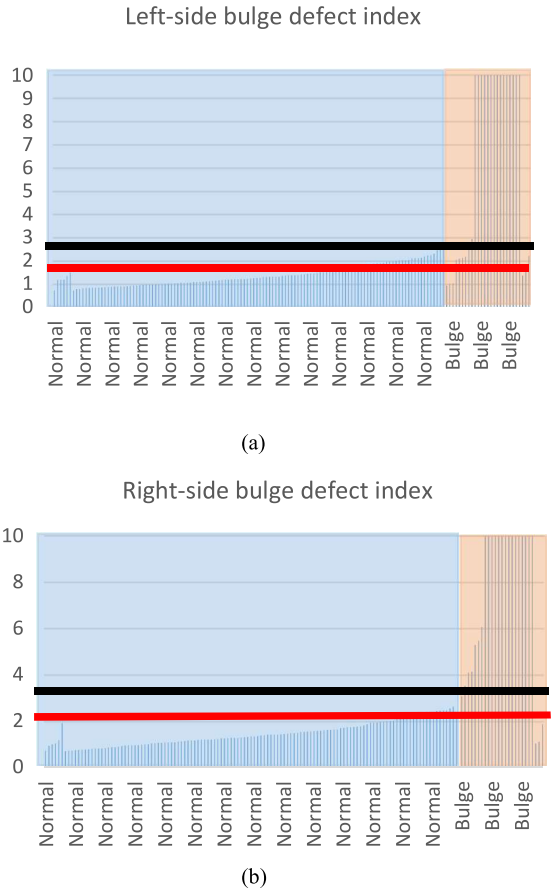

Fig.10. The measurement result of bulge defect. (a) The histogram of left-side bulge defect index, (b) The histogram of right-side bulge index. The light blue area is the normal-package results; light red area is the bulge-packagesresults. The red line is the decision threshold value, and the black line is the buffer threshold value.

References

[1] W.-C. Wang, S.-L. Chen, L.-B. Chen, and W.-J. Chang, "A machine vision based automatic optical inspection system for measuring drilling quality of printed circuit boards," IEEE Access, vol.5, pp.10817-10833, Nov. 2016.

[2] J. Richter, D. Streitferdt, and E. Rozova, "On the development of intelligent optical inspections," in Proc. 2017 IEEE 7th Annual Computing and Communication Workshop and Conference, Jan. 2017.

[3] S.-H. Huang and Y.-C. Pan, "Automated visual inspection in the semiconductor industry: A survey," Computer in Industry, no. 66, pp. 1-10, 2015.

[4] M. Shi, R. Fu, Y. Guo, Sh. Bai, and B.Xu, "Fabric defect detection using local contrast deviations," Multimedia Tools and Applications, no. 52, pp. 147-157, 2011.

JOIN US AT THE NEXT EI!

IS&T International Symposium on

Electronic Imaging

SCIENCE AND TECHNOLOGY

Imaging across applications . . . Where industry and academia meet!

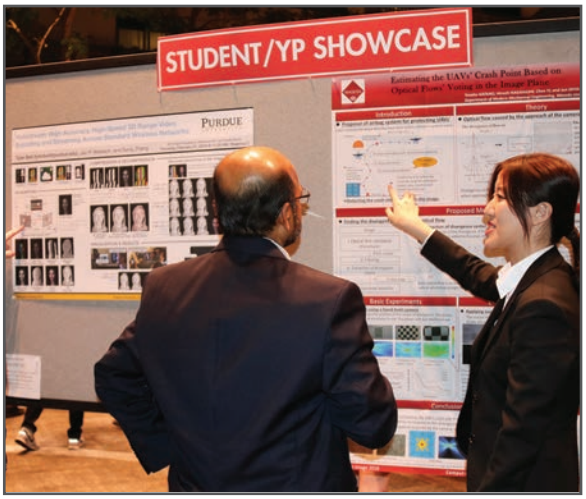

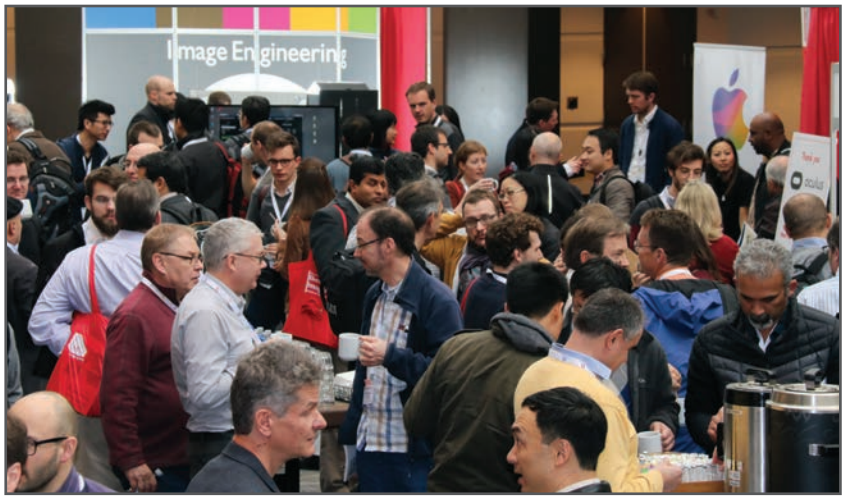

• SHORT COURSES • EXHIBITS • DEMONSTRATION SESSION • PLENARY TALKS •
• INTERACTIVE PAPER SESSION • SPECIAL EVENTS • TECHNICAL SESSIONS •

www.electronicimaging.org

IS&T
imaging.org